nature neuroscience

Flexible strategies for sensory integration during motor planning

Samuel J Sober & Philip N Sabes

When planning target-directed reaching movements, human subjects combine visual and proprioceptive feedback to form two estimates of the arm's position: one to plan the reach direction, and another to convert that direction into a motor command. These position estimates are based on the same sensory signals but rely on different combinations of visual and proprioceptive input, suggesting that the brain weights sensory inputs differently depending on the computation being performed. Here we show that the relative weighting of vision and proprioception depends both on the sensory modality of the target and on the information content of the visual feedback, and that these factors affect the two stages of planning independently. The observed diversity of weightings demonstrates the flexibility of sensory integration and suggests a unifying principle by which the brain chooses sensory inputs so as to minimize errors arising from the transformation of sensory signals between coordinate frames.

Information about a single environmental cue or variable is often available to more than one sensory modality, raising the question of how the brain weights and combines sensory signals during perception and behavior. Previous theories of how this is accomplished have focused on the statistical properties of the individual sensory signals[1–5]. Here we demonstrate that input statistics alone are insufficient to explain sensory integration during motor planning. Rather, we provide evidence that sensory integration is strongly influenced by the cost of performing coordinate transformations on sensory inputs. The results suggest a model in which sensory signals are weighted to limit the errors that are introduced when these signals are transformed between coordinate frames.

We have previously developed a method for studying the integration of visual and proprioceptive feedback signals from the arm during the planning of reaching movements[6]. Subjects reached to visual targets in a virtual visual feedback environment. We quantified the relative weighting of vision and proprioception by displacing the virtual visual feedback and measuring the resulting reach errors. Such shifted feedback introduces two types of error: a 'movement vector' (MV) error that arises when the location of the visual target is compared with the position of the fingertip (**Fig. 1a**) and an 'inverse model' (INV) error that arises when the planned direction is converted into an intrinsic (muscle- or joint-based) motor command (**Fig. 1b,c**). Although errors from both of these stages can affect a single movement, the MV error (**Fig. 1d**) and INV error (**Fig. 1e**) can be separately inferred from the pattern of shift-induced errors measured across multiple reaches in different directions (**Fig. 1f**). Furthermore, the magnitude of each type of error is proportional to the reliance on the shifted visual feedback at each planning stage. By fitting these shift-induced error patterns with a simple model of motor planning, we determined the relative weighting of visual feedback at each planning stage. We found that the two stages of reach planning rely on very different mixtures of visual and proprioceptive input: movement vector planning relies mostly on visual signals, whereas computation of the intrinsic motor command relies more on proprioceptive signals[6].

Here we address the question of why the same sensory signals are weighted so differently at the two stages of reach planning. We suggest that the difference previously observed[6] was due to the coordinate frame in which the two computations took place. In that study, subjects reached to visual targets, and the visual feedback reflected only the position of the fingertip. Planning the movement vector required an estimate of the current position of the fingertip relative to the visual target, a simple vector subtraction in visual coordinates. In contrast, computation of the motor command required an estimate of the intrinsic state of the arm, which was encoded by proprioceptive afferents but was not explicitly represented by the visual feedback. The sensory signals that were not already in the appropriate coordinate frame for each stage of planning would have had to undergo a transformation in order to be used in the relevant computation. We hypothesize that the weighting of vision and proprioception reflects a strategy of minimizing errors that arise during such coordinate transformations. We tested this idea in two experiments, altering either the coordinate frame of the target or the nature of the visual feedback.

We first examined whether sensory integration during movement vector planning is influenced by the sensory modality of the target (Experiment 1). During reaching to a visual target, the nervous system might rely more on vision because visual feedback from the arm is already in the target's coordinate frame. Before proprioceptive signals can be used, they must be transformed into visual coordinates. This transformation will incur errors, either because of biases in the

Department of Physiology, W.M. Keck Foundation Center for Integrative Neuroscience and Neuroscience Graduate Program, University of California, San Francisco, San Francisco, California 94143-0444, USA. Correspondence should be addressed to P.S. (sabes@phy.ucsf.edu).

Published online 27 March 2005; doi:10.1038/nn1427

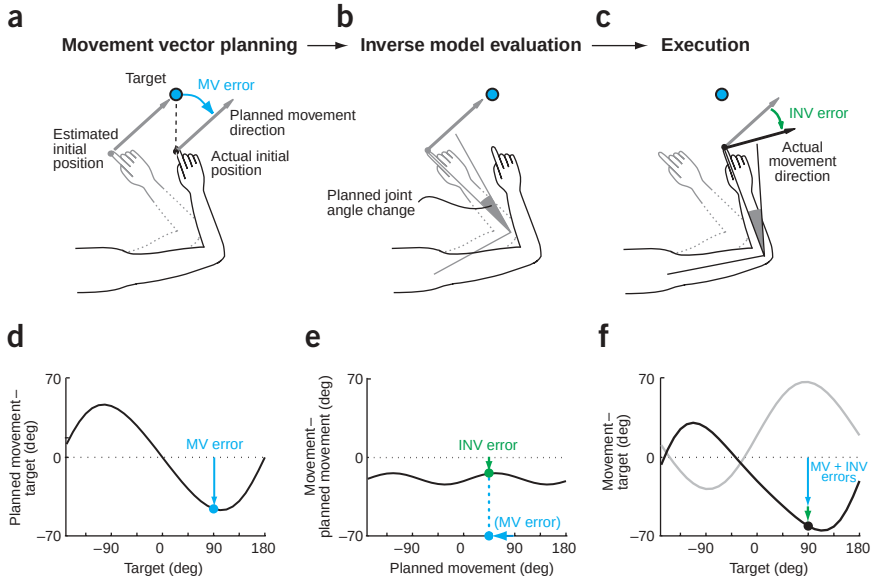

Figure 1 Two types of reaching errors induced by shifted visual feedback. (**a**) Error in planned movement direction resulting from a leftward error in the position estimate used to plan the movement vector ('MV error'). This error is caused by a leftward shift of the visual feedback. The planned movement direction for a reach to the target at 90° (blue dot) differs from the true hand-to-target direction, resulting in a clockwise error (blue arrow). (**b**,**c**) Error in initial movement direction resulting from a leftward error in the position estimate used to evaluate the inverse model of the arm and compute the motor command ('INV error'). The wrong joint-angle displacement (motor command) is planned for the desired movement vector (**b**), resulting in a movement error (**c**). (**d**) The bimodal MV error pattern resulting from a leftward error in estimated position. Blue arrow, MV error shown in **a**. (**e**) A leftward error in estimated position results in clockwise errors for all target directions. (**f**) Measured errors in initial direction are a combined effect of MV and INV errors (black curve). A rightward error in position estimates would produce an error pattern of opposite sign (gray curve). Here and in later figures, 0° refers to a rightward vector, and positive angles are counterclockwise.

mapping between coordinate frames or because of variance introduced by the additional computation[7,8], and the effect of these errors will scale with the relative weighting of the proprioceptive signal. Thus, if a proprioceptive target (here the felt location of the other hand underneath the tabletop) were used instead of a visual target, we predict that subjects would rely more on proprioceptive feedback from the reaching arm, as the target would already be in an intrinsic coordinate frame. This change would be reflected as a reduction in the MV error observed when the visual feedback is shifted (model data illustrating this prediction are shown in **Fig. 2a**).

We next asked whether the information content of the visual feedback influences sensory integration (Experiment 2). We hypothesized that the previously observed reliance on proprioception during motor command generation was due in part to the fact that the visual feedback (a single spot of light) specified only the position of the fingertip[6], whereas an estimate of the joint angles was required to compute the appropriate motor command from the desired movement vector (**Fig. 1b**). The transformation of visual fingertip feedback into joint angles is expected to incur errors, again as a result of inaccuracies in the mapping or of the introduction of variance during the computation. In addition, this transformation is particularly prone to errors, as it is generally underconstrained: a single fingertip location can be achieved by many joint angle configurations when the arm's range of motion is unrestricted. The reliance on proprioception in this context could reflect a general strategy of avoiding an underconstrained sensory transformation, even though the arm was actually restricted to two degrees of freedom in these experiments. In contrast, if the virtual visual feedback explicitly represented joint angles as well as fingertip location, this source of uncertainty would be eliminated, and the errors due to the transformation would be reduced. We therefore predicted that if the visual feedback included an image of the reaching arm (and hence explicit information about joint angles), subjects would rely more on vision during motor command generation. This in turn would lead to greater INV error when the visual feedback was shifted (model data shown in **Fig. 2b**).

We measured the changes in MV and INV error induced by the two manipulations outlined above. In both cases, we observed the predicted changes in the relative weighting of vision and proprioception. These task-dependent changes seem to affect the two planning stages independently, suggesting that sensory integration is a local process influenced by the particular computations performed at each planning stage.

RESULTS

We tested the predictions described above in two separate experiments. In both studies, subjects made planar reaching movements on a horizontal table with virtual visual feedback (**Fig. 3a**). Visual feedback was provided as subjects planned reaches but was extinguished at reach onset.

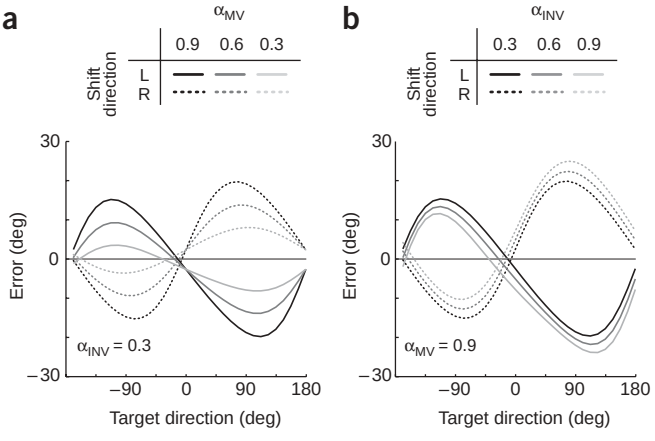

Figure 2 Predicted changes in Experiments 1 and 2. Each panel shows the movement-direction errors predicted for different values of α_{MV} and α_{INV}, which represent the relative weighting of visual feedback at the first and second stages of reach planning, respectively (see Methods). Both panels include the model predictions for $\alpha_{MV} = 0.9$, $\alpha_{INV} = 0.3$ (black lines), corresponding to the values expected for reaches to a visual target with fingertip feedback[6]. (**a**) Proprioceptive targets in Experiment 1 are expected to result in a lower value of α_{MV}. (**b**) Arm feedback in Experiment 2 is expected to result in a higher value of α_{INV}.

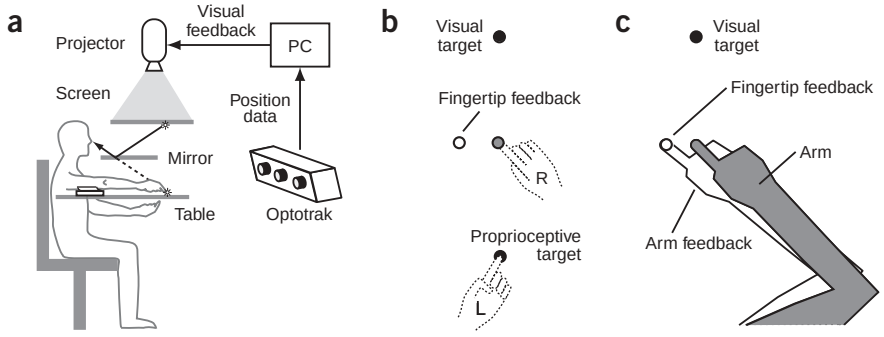

Figure 3 Data collection and task parameters. (**a**) Virtual visual feedback setup. (**b**) In Experiment 1, a visual and a proprioceptive target were both present on every trial; the 'go' signal cued subjects which reach to make. Visual feedback of the fingertip position was either veridical (gray dot) or shifted leftward (white dot) or rightward by 6 cm. (**c**) In Experiment 2, subjects reached to visual targets with visual feedback that showed either the fingertip or a simple, polygonal rendering of the arm. Visual feedback either reflected the true position of the fingertip or was shifted leftward (white dot, polygon) or rightward by 7 cm.

Effects of target modality

In Experiment 1, two targets were available on each trial: a visual target, consisting of a spot of light, and a proprioceptive target, provided by the felt position of the left index fingertip (**Fig. 3b**). The left hand was positioned beneath the table so that the two hands never came into contact. The color of the 'go' signal instructed subjects whether to reach to the visual or proprioceptive target. This instruction was randomized across trials. Data from a typical subject are illustrated in **Figure 4**. For both target types, raw reach trajectories show the effects of shifted visual feedback (**Fig. 4a**). For example, reaches made with leftward feedback shifts show rightward directional errors, consistent with a leftward error in estimated hand position during movement vector planning. Additionally, the effects of the visual shifts were smaller when the subject reached to proprioceptive targets, consistent with our hypothesis that subjects would rely less on visual feedback in this trial type. Reaction times, movement times, and baseline reach trajectories were qualitatively similar for visual-target and proprioceptive-target reaches, although reaches to proprioceptive targets were more variable and tended to be hypometric (**Supplementary Note** online).

In quantifying the errors that were due to pre-movement exposure to shifted visual feedback, we focused on the direction of movement just after reach onset, as this variable reflects the movement plan and not online feedback corrections. We computed shift-induced errors by subtracting the initial movement direction on baseline trials from the initial movement direction on trials that included shifts of the visual feedback. The sample subject's shift-induced errors (**Fig. 4c**) resembled the model predictions (**Fig. 2a**).

We inferred the relative weighting of vision and proprioception at each planning stage using a simple mathematical model of motor planning. For the model to make specific predictions, it must include assumptions about the particular form in which the brain encodes motor commands. In the present model, we assume that the motor command specifies the joint angle velocities (**Fig. 1b**), although an alternate model is considered below. We quantified sensory integration by fitting two model parameters, α_{MV} and α_{INV}, that represent the relative weighting of vision when computing the movement vector and the intrinsic motor command, respectively ($\alpha = 0$ for proprioception only and $\alpha = 1$ for vision only; see Methods).

We performed this analysis separately for the visual-target and proprioceptive-target data shown in **Figure 4c**, and the model fits are shown as dotted lines. For this subject, the best-fit weighting parameters were $\alpha_{MV} = 0.96$, $\alpha_{INV} = 0.32$ for visual-target trials and $\alpha_{MV} = 0.49$, $\alpha_{INV} = 0.19$ for proprioceptive-target trials. This subject therefore relied almost entirely on visual feedback ($\alpha_{MV} = 0.96$) when computing the movement vector to visual targets, but relied roughly equally on visual and proprioceptive information ($\alpha_{MV} = 0.49$) when planning the movement vector to proprioceptive targets.

We observed this same trend when directional data were averaged across the seven subjects in Experiment 1 (**Fig. 5**). Shift-induced errors

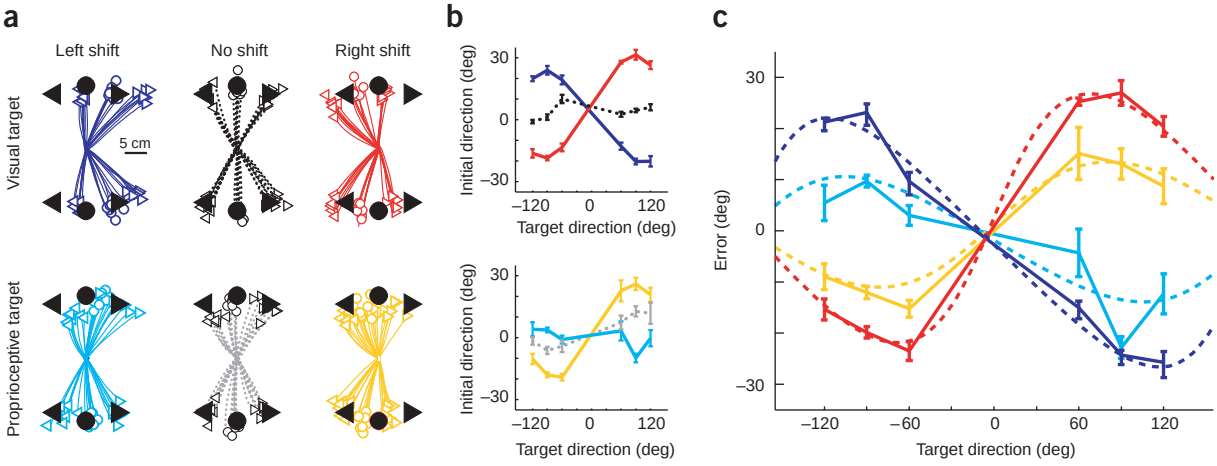

Figure 4 Sample data, Experiment 1. (**a**) Raw reach trajectories for a representative subject. Filled symbols, reach targets; corresponding open symbols, reach endpoints. (**b**) Initial reach direction with respect to target direction, using the color conventions of **a**. (**c**) Reach errors induced by visual feedback shifts, computed by subtracting the baseline directional biases (dotted lines in **b**) from the initial directions in the shifted conditions (solid lines in **b**). Dashed lines, model fits. Best-fit weighting parameters: $\alpha_{MV} = 0.96$, $\alpha_{INV} = 0.32$ for visual-target reaches and $\alpha_{MV} = 0.49$, $\alpha_{INV} = 0.19$ for proprioceptive-target reaches. Error bars, ± 1 s.e.m.

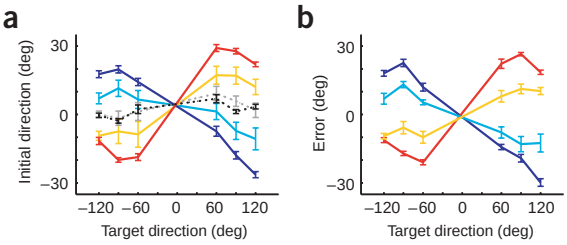

Figure 5 Group data, Experiment 1. (**a**) Average initial direction (±1 s.e.m.), with respect to target direction, for visual- and proprioceptive-target reaches. (**b**) Average errors in initial direction (±1 s.e.m.). Color conventions as in **Figure 4**.

were larger during reaching to visual targets, showing a decreased reliance on vision during reaching to proprioceptive targets. We quantified this effect by the fit values of α_{MV} and α_{INV} (**Fig. 6**). Every subject showed a significant ($P < 0.05$) reduction in α_{MV} when reaching to proprioceptive targets (mean $\alpha_{MV} = 0.88$, visual-target trials; mean $\alpha_{MV} = 0.42$, proprioceptive-target trials). The mean decrement in α_{MV} of 0.46 corresponds to a nearly fivefold increase in the use of proprioceptive information in the proprioceptive-target condition. There was also a small reduction in α_{INV} (mean, 0.17), which was significant in a single subject (the completely filled circle in **Fig. 6c**). The weighting of feedback signals during movement vector planning therefore depends critically on the sensory modality of the target.

The analysis described above assumes that motor commands are planned in terms of joint angle velocity, a purely kinematic variable. As it is an open question whether the brain plans reaching movements in terms of kinematic or dynamic variables[9–12], we also considered a second model in which the motor command specifies the joint torques (see Methods). This torque command model yielded results very similar to the original velocity command model (mean decrements in α_{MV} and α_{INV} of 0.48 and 0.18, respectively). The close agreement between these two models suggests that our ability to quantify sensory integration is independent of whether motor commands are specified kinematically or dynamically, consistent with our earlier findings[6].

Controls for transfer effects and non-proprioceptive cues

Three issues regarding the design of Experiment 1 warranted control studies. First, although subjects received shifted visual feedback from only the reaching (right) hand, it is possible that the shifted visual feedback could have affected the felt position of the target (left) hand. Analogous intermanual transfer has been described in studies of visuomotor adaptation[13–16], although such effects are not always present[17–20]. In a separate experiment, we demonstrated that the visual shift protocol used in Experiment 1 did not affect the felt position of the left hand (**Supplementary Note**).

Second, the direction of gaze was neither measured nor constrained in Experiment 1. This is potentially problematic, as subjects could have determined the target location for proprioceptive reaches using either a visual fixation point or the felt gaze direction, rather than the proprioceptive signals from the left arm. To address this concern, we repeated Experiment 1 with the additional constraint that subjects were required to maintain visual fixation on one of a number of points near the center of the workspace (**Supplementary Note**). We found that the task-dependent changes in α_{MV} and α_{INV} were very similar whether or not gaze was constrained. We conclude that any information provided by gaze direction had a minimal effect on sensory integration during reach planning.

A third potential confound in the proprioceptive-target condition is that subjects actively positioned the left arm and were required to support it against gravity during reach planning. Therefore, efference copy could have provided non-proprioceptive information about the position of the left arm. To ensure that this factor did not account for our results, we tested subjects on another variation of Experiment 1 in which the left arm was passively moved to the target location and was supported by a second tabletop throughout the trial. The task-dependent change in α_{MV} when the target arm was passively supported was of comparable magnitude to that observed in the original experiment (**Supplementary Note**). Changes in α_{MV} therefore do not depend on the use of non-proprioceptive cues to the location of the proprioceptive target.

Effects of visual feedback type

In Experiment 2, we tested the hypothesis that subjects would rely more on vision during inverse model evaluation if the visual feedback represented the arm, and thus the configuration of the joints, rather than just the location of the fingertip. All reaches were to visual targets, and feedback consisted of either a spot specifying fingertip location or a simple virtual image of the arm (**Fig. 3c**). **Figure 7a,b** shows data from a single subject. The bimodal MV error pattern was similar in the two feedback conditions. Averaging across targets for each shift direction showed the INV error pattern: reaches made with leftward shifts were biased clockwise, whereas reaches with rightward shifts were biased counterclockwise. This INV error pattern was more pronounced in the arm-feedback condition in the sample subject (compare the dashed lines in **Fig. 7a,b**), as in the rest of the subject pool (**Fig. 7c**). These data suggest that subjects rely more on vision when computing the intrinsic motor command when the visual feedback specifies the posture of the arm.

We quantified this effect by fitting the weighting parameters to the data from fingertip- and arm-feedback reaches. Model fits for the sample subject (**Fig. 7a,b**) yielded values of $\alpha_{MV} = 0.84$, $\alpha_{INV} = 0.25$ for fingertip-feedback trials and $\alpha_{MV} = 0.79$, $\alpha_{INV} = 0.54$ for arm-feedback trials (gray symbols in **Fig. 8a,b**). Thus, for this subject, visual feedback was weighted 25% during the second stage of reach planning when the

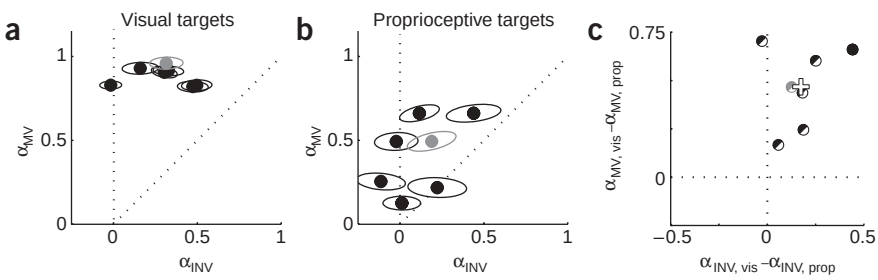

Figure 6 Model fits, Experiment 1. (**a**,**b**) Fit values of α_{MV} and α_{INV} for reaches to visual and proprioceptive targets, respectively. Ellipses represent 1 s.e.m. Dotted lines, $\alpha_{INV} = \alpha_{MV}$ and $\alpha_{INV} = 0$. (**c**) Differences in model fit between visual- and proprioceptive-target reaches. The top left half of the symbol is filled if the task-dependent change in α_{MV} is significant (permutation test, $P < 0.05$), and the lower right half is filled if the change in α_{INV} is significant. +, average across subjects. In all plots, the gray symbols are for the sample subject shown in **Figure 4**.

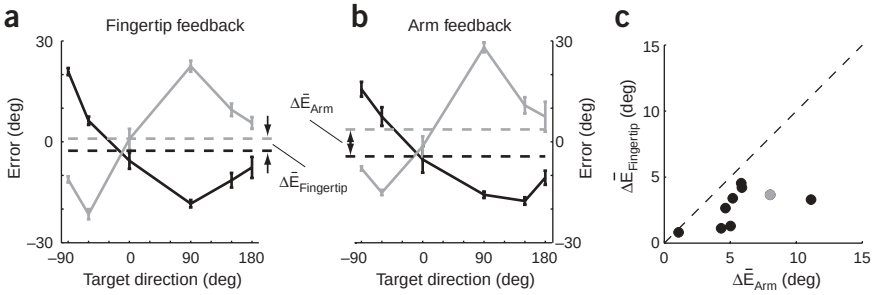

Figure 7 Sample and group data, Experiment 2. (**a**,**b**) Data from a representative subject in the fingertip-feedback and arm-feedback conditions, respectively. Gray, rightward visual shift; black, leftward visual shift; dashed lines, mean error across the six target directions. Error bars, ±1 s.e.m. Arrows indicate $\Delta\bar{E}$, the difference between the mean errors for rightward- and leftward-shifted visual feedback. (**c**) Differences in mean errors for all subjects. Gray dot, sample subject whose data are shown in **a** and **b**; dashed line, $\Delta\bar{E}_{Arm} = \Delta\bar{E}_{Fingertip}$.

feedback represented fingertip position only. However, when visual feedback consisted of an image of the arm, that contribution increased to 54%. For all subjects, α_{INV} was greater during the arm-feedback trials (mean $\alpha_{INV} = 0.24$, fingertip feedback; $\alpha_{INV} = 0.42$, arm feedback), although this difference was significant in only three out of ten subjects (**Fig. 8c**). The mean change in α_{INV} of 0.18 across feedback conditions corresponded to a 75% increase in the use of visual information in the arm-feedback condition. In contrast, the mean change in α_{MV} due to the use of arm feedback was −0.01. As was the case in Experiment 1, the torque command model produced similar results as the original velocity command model, yielding average changes in α_{INV} and α_{MV} of 0.28 and 0.02, respectively.

DISCUSSION

We have shown that altering the details of a sensorimotor task changes the relative weighting of visual and proprioceptive feedback used to plan the motor response. These changes can occur on a trial-to-trial basis as task conditions are varied. Furthermore, the task variations used in Experiments 1 and 2 drive different changes in weighting at the two stages of reach planning, suggesting a degree of independence in sensory integration at these stages.

Our results show that sensory integration is not determined solely by the statistics of the sensory input but is also significantly influenced by the computations required for task execution. The observed pattern of changes reflects a reduced reliance on signals that must be transformed between visual and proprioceptive coordinate frames. There are several potential costs that could be minimized by avoiding transformed signals: for example, the metabolic cost of performing additional neural computations. However, we propose that sensory signals are weighted in order to minimize errors resulting from inherently noisy coordinate transformations. This points to a view of sensory integration as a set of local, independently controlled processes optimized to improve sensorimotor performance.

In Experiment 1, the value of α_{MV} depended on the sensory modality of the target, suggesting that the brain weights sensory feedback so as to minimize the adverse effects of transforming arm position signals into the coordinate frame of the target. Control studies demonstrate that these effects on α_{MV} are not the result of intermanual transfer of the visual shift, the effects of gaze direction, or the use of an active motor command to position the proprioceptive target. One remaining question is why this effect was not symmetrical: when reaching to visual targets, visual feedback was weighted almost 90%, whereas proprioception was weighted just over 50% when reaching to the fingertip of the other hand. This asymmetry may be due to the fact that when reaching to the proprioceptive target, an additional transformation is required to convert proprioceptive signals from the left arm into the intrinsic coordinates of the right arm.

Another issue that arises from Experiment 1 is why α_{INV} decreases during reaching to proprioceptive targets. This effect was not predicted, as the target location was used only to compute the movement vector (see the schematic of **Fig. 1**). Although this effect was smaller than the change in α_{MV}, the trend was seen in all but one subject. One possible explanation is that these parallel changes in α_{MV} and α_{INV} result from attentional shifts, which have previously been shown to affect sensory integration[21,22]. A shift of attentional focus from vision to proprioception could potentially underlie the decreases in both α_{MV} and α_{INV}, despite the fact that the latter change is much smaller. However, Experiment 1 was explicitly designed to reduce the likelihood of such attentional shifts: visual-target and proprioceptive-target trials were randomly interleaved, every trial included both a visual and a proprioceptive target, and subjects were not instructed which target to reach to until shortly before the 'go' signal (see Methods). Furthermore, attentional effects alone cannot explain key components of our results: vision and proprioception each dominated at different planning stages during the same movement (**Figs. 6** and **8**), and in Experiment 2, α_{INV} increased without consistent changes in α_{MV} (**Fig. 8c**).

Another possibility is that the coordinate frame of the planned movement vector is different in the two tasks. Movement vectors might be computed in visual coordinates when reaching to visual targets, but in an intrinsic (or intermediate) coordinate frame when reaching to proprioceptive targets. The computations required at the INV stage

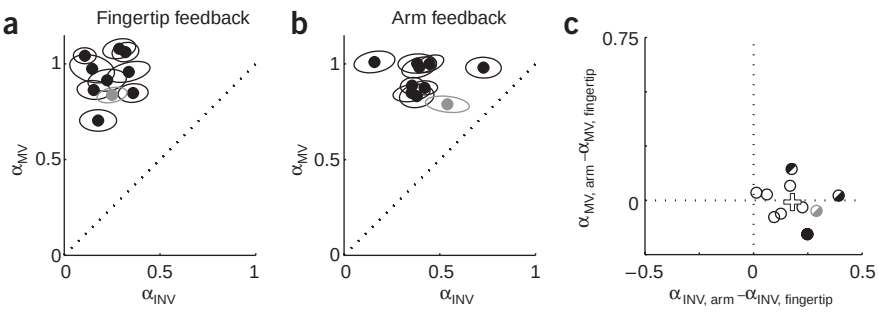

Figure 8 Model fits, Experiment 2. (**a**,**b**) Fit values of α_{MV} and α_{INV} for fingertip-feedback and arm-feedback trials, respectively. (**c**) Differences in model fit between arm- and fingertip-feedback reaches. In all plots, the gray dot represents the subject whose data is shown in **Figure 7a**,**b**. Other plotting conventions as in **Figure 6**.

could therefore differ in the two tasks, resulting in the observed changes in α_{INV}. In any case, these potential differences do not affect the model's predictions about sensory integration during movement vector planning or our interpretation of the observed changes in α_{MV}.

Experiment 2 demonstrates that the value of α_{INV} depends on the information content of the visual feedback. When the visual feedback represents only the fingertip position, proprioception dominates during the computation of the motor command. We propose that this reflects an error-minimization strategy, as determination of the posture of the arm from the visually perceived fingertip location is an ill-posed problem, and thus prone to errors. Indeed, when visual feedback of the whole arm is available, the two sensory modalities contribute nearly equally to the computation of the motor command. In contrast, movement vector planning seems to be insensitive to the type of visual feedback. This supports our interpretation that the key difference between the two feedback conditions is the information about the configuration of the joints, rather than the size or salience of the visual stimulus.

Our results indicate that simple minimum-variance models of sensory integration, in which the weighting of sensory signals is determined solely by their input statistics, are incomplete. The minimum-variance principle has successfully described sensory integration in a wide variety of tasks[2–5]; however, it is inconsistent with our finding that the same sensory signals can be given very different weightings at different stages of reach planning or at the same stage of planning in different tasks. As noted above, these effects suggest a strategy of minimizing the role of sensory signals that have undergone coordinate transformations. Our results are thus consistent with an extended minimum-variance model that accounts for the variability that can arise during noisy coordinate transformations.

The experiments presented here demonstrate for the first time that sensory integration during reach planning is a dynamic process driven by the computational demands of the task. These psychophysical phenomena presumably reflect differences in the neural circuits or patterns of activity that are engaged during task performance. Neurons in many of the cortical areas involved in reach planning receive both visual and proprioceptive inputs[23–26]. Our results suggest that these sensory inputs are gated in a task-dependent way. By quantifying the mixture of visual and proprioceptive inputs to a neural population across the task manipulations described above, it may be possible to determine the computation in which a group of neurons is participating. Such studies will help bridge the gap between computational and physiological descriptions of motor planning.

METHODS

This study was approved by the University of California, San Francisco Committee on Human Research, and subjects gave written informed consent. All subjects were right-handed, 18–34 years of age, and healthy, with normal or corrected-to-normal vision. Subjects were naive to the purpose of the experiments and were paid for their participation. Seven subjects (five women, two men) participated in Experiment 1, and ten different subjects (five women, five men) participated in Experiment 2.

Experimental setup and data collection. Visual targets and visual feedback of the arm were presented using a virtual reality display system described previously[6] (**Fig. 3a**). Arm position was monitored with an infrared position tracking device (Optotrak 3020, Northern Digital). Reaches were performed with the right arm, which rested on a table at shoulder height. A custom-built splint immobilized the wrist joint and fixed the right index finger in an extended position. An air sled under the upper arm minimized friction between the arm and the table. The torso was restrained using a vest attached to the subject's chair. This arrangement restricted the arm to two degrees of freedom such that arm position could be expressed interchangeably as x, a two-dimensional vector representing the cartesian position of the fingertip on the table, or as θ, a two-dimensional vector representing the elbow and shoulder angles.

General task design. In both experiments, reaches began from a start point located approximately 40 cm from the chest along the midline. At the beginning of each trial, visual feedback from the reaching arm reflected either the true location of the fingertip or a location shifted to the left or right. Rightward, leftward and null shifts were randomly interleaved to prevent sensorimotor adaptation. The visual feedback disappeared after reach onset once the fingertip moved 5 mm from the start point. Subjects received a numerical score based on their performance on each trial (**Supplementary Note**). After the experiment, subjects were asked about the accuracy of the visual feedback. All subjects reported being unaware of a visual shift.

Task design, Experiment 1. In Experiment 1, we varied the sensory modality of the reach target (**Fig. 3b**). On half of the trials ('visual-target trials'), subjects reached to a visual target consisting of a red dot 5 mm in diameter. On the other trials ('proprioceptive-target trials'), subjects reached to the felt location of their left index finger, which had been positioned below the tabletop. Each trial included one visual target and one proprioceptive target. Targets were selected randomly on each trial from six possible locations (14 cm from the start point at 60°, 90°, 120°, −120°, −90° or −60° with respect to the rightward axis; **Fig. 4a**). These directions were chosen to maximize the statistical power of the model when fitting α_{MV}. The visual and proprioceptive targets were always 180° apart, as in **Figure 3b**. On all trials, visual feedback of the right index fingertip consisted of a white, 5-mm-radius spot that appeared either at the fingertip or shifted leftward or rightward by 6 cm.

At the beginning of each trial, subjects positioned their right fingertip in order to place the feedback spot within an 8-mm ring. The feedback spot was visible only when the y-coordinate of the fingertip (defined as the axis pointing toward or away from the body) was within 8 mm of the y-coordinate of the start point. Once the starting position was achieved, the ring disappeared and an array of nine arrows appeared at a randomly selected location. The arrows were used to guide the left index finger to the preselected location of the proprioceptive target: the direction and magnitude of the arrows were continuously adjusted to indicate the direction and (scaled) distance from the left fingertip to the target location. When the fingertip had moved to within 5 mm of the target location, the arrows disappeared and the visual target appeared at a location distinct from the start point and the proprioceptive target (**Fig. 3b**). After a delay of 500–1,500 ms, an instruction cue appeared in the form of a small colored dot on top of the feedback spot. Subjects reached to the visual target if this dot was red and to the proprioceptive target if the dot was blue. The target instruction cue remained illuminated for 1,400–1,600 ms, and its disappearance served as the 'go' signal, cueing the subject to begin the reach with the right arm. Subjects were required to hold the left index fingertip at the proprioceptive target throughout the reaching movement. All subjects did so successfully on every trial (the left index fingertip never moved more than 1 cm; mean fingertip excursion <1 mm).

Eight reaches were made to each of the six targets with each of the three visual shifts, totaling 144 reaches each in the visual- and proprioceptive-target conditions. Trial order was randomized across all factors. A set of 36 familiarization trials preceded the experiment and included all six trial types. Visual feedback was unshifted during familiarization trials, but the starting location of some trials was shifted 6 cm to the left or right of midline in order to familiarize subjects with reaches that appeared to originate from three different start points. Familiarization trials were not included in the subsequent analyses.

Task design, Experiment 2. In Experiment 2, we varied the information content of the visual feedback (**Fig. 3c**). In half of the trials ('fingertip-feedback trials'), the visual feedback from the right arm consisted of a bright white spot (100% gray level), as in Experiment 1, and feedback was either veridical or shifted right or left by 7 cm. In the other half of trials ('arm-feedback trials'), the visual feedback consisted of a white polygon (60% gray level) in the shape of the subject's arm. Either the arm feedback was coextensive with the subject's arm or the virtual fingertip was shifted left or right by 7 cm. When the fingertip

was shifted, the arm feedback was displayed with the posture that would have achieved the shifted fingertip location given the true position of the subject's shoulder.

At the beginning of a trial, subjects used visual feedback to position their right index fingertip at the start point, as in Experiment 1. In Experiment 2, however, visual feedback appeared only after the *y*-coordinate of the fingertip was within 3 cm of starting value. When the visual feedback was within the start window, a visual target consisting of a red dot of radius 5 mm appeared. Target location was selected randomly on each trial from one of six positions (18 cm from the start point at 0°, 90°, 150°, 180°, −90° and −60°). These targets were chosen to maximize the statistical power of the model when fitting α_{INV}. After a delay of 500–1,500 ms, a small red dot appeared on top of the visual feedback spot (fingertip-feedback trials) or the tip of the virtual finger (arm-feedback trials). After 1,400–1,600 ms the red dot disappeared, signaling the subject to 'go'. Subjects did not use their left hands in Experiment 2.

For each type of visual feedback, eight reaches were made to each of the six targets with the three visual shifts, and the order of the 144 trials was randomized. Trials for the two feedback conditions were presented in separate blocks, with block order randomized across subjects. Block order had no effect on reach kinematics or the results or the model fits. Each block began with 36 familiarization trials as in Experiment 1.

Trajectory analysis. Position data were smoothed with a low-pass Butterworth filter (cutoff frequency of 6 Hz), and fingertip velocity was then computed using first-order numerical differentiation. Initial reach direction was quantified as the angle of the instantaneous velocity when the velocity magnitude first exceeded 40% of its peak value. This landmark fell 82 ± 18 ms (mean ± average within-subject s.d.) after reach onset in Experiment 1 and 94 ± 19 ms after reach onset in Experiment 2.

Modeling the initial movement direction. We have developed a method for quantifying the relative reliance on vision and proprioception during reach planning[6], which we applied to the data from Experiments 1 and 2. Work from our and other labs has shown that subjects form two estimates of arm position when planning a reaching movement[6,27–30]. Briefly, we assume that the two arm position estimates, $\hat{x}_{MV}$ and $\hat{x}_{INV}$, are weighted combinations of visual ($\hat{x}_{vis}$) and proprioceptive ($\hat{x}_{prop}$) inputs:

$$\hat{x}_{MV} = \alpha_{MV}\hat{x}_{vis} + (1 - \alpha_{MV})\hat{x}_{prop} \quad (1)$$

$$\hat{x}_{INV} = \alpha_{INV}\hat{x}_{vis} + (1 - \alpha_{INV})\hat{x}_{prop} \quad (2)$$

The estimate $\hat{x}_{MV}$ is used to calculate the desired initial fingertip velocity $\dot{x}^*$, the 'movement vector'. The direction of this vector is determined by

$$\angle\, \dot{x}^* = \angle\, (x_d^* - \hat{x}_{MV}) + \omega_d \quad (3)$$

where $\angle\, z$ represents the angle of any vector z, x^* represents the target location, ω is an angular offset term that captures directional biases in baseline reaches, and $d \in [1, ..., 6]$ indexes x^* and ω over the six targets. Note that the error in $\hat{x}_{MV}$ and $\angle\, x^*$ due to shifted visual feedback (MV error) scales with α_{MV} (**Fig. 2a**).

The desired fingertip velocity $\dot{x}^*$ is then used to compute the motor command, specified as a vector of joint angle velocities $\dot{\theta}$:

$$\dot{\theta} = J^{-1}(\hat{\theta}_{INV})\dot{x}^* \quad (4)$$

where $\hat{\theta}_{INV} = K^{-1}(\hat{x}_{INV})$ is calculated from the inverse kinematics function K^{-1} that describes the mapping from cartesian fingertip location to joint angles, and

$$J(\theta) = \frac{dx}{d\theta}$$

is the Jacobian of the arm. This computation represents an inverse model of the arm[31].

When the motor command is executed, the fingertip moves with an initial velocity described by

$$\dot{x} = J(\theta)\dot{\theta} = [J(\theta)J^{-1}(\hat{\theta}_{INV})]\dot{x}^* \quad (5)$$

Note that shifting the visual feedback will cause a discrepancy between $\dot{x}$ and $\dot{x}^*$, as the matrix $J(\theta)J^{-1}(\hat{\theta}_{INV})$ will equal the identity matrix only when $\theta = \hat{\theta}_{INV}$. The size of this INV error increases with increasing α_{INV} (**Fig. 2b**). Finally, as equation (3) specifies only the direction of $\dot{x}^*$, the predicted direction of only the initial movement vector in equation (5) is fit to empirical data.

The velocity command model, described in equations (1)–(5), assumes that the movement vector is specified as a desired initial velocity of the fingertip ($\dot{x}^*$) and that the motor command consists of joint angle velocities ($\dot{\theta}$). We have previously shown that similar fit values of α_{MV} and α_{INV} are obtained with an alternate model in which the movement vector is specified as the desired initial acceleration of the fingertip and the motor command consists of joint torques. This torque command model[6] takes into account the inertial properties of the arm. Data from Experiments 1 and 2 were fit with both models. See ref. 6 for a fuller description of these models.

Fitting model predictions to the data. We fit the two free parameters of the model, α_{MV} and α_{INV}, to the data from each subject and experimental condition with a nonlinear regression algorithm (nlinfit in MATLAB, Mathworks). The values of $\hat{x}_{vis}$ and $\hat{x}_{prop}$ in the model were set to the position of the visual feedback and the true position of the fingertip, respectively, on each trial. The value of x^* was set to the target position. The baseline bias terms (ω_d in equation (3)) were determined from the mean angular difference between the target direction and the initial velocity direction in trials with unshifted feedback.

We used permutation tests[32] to evaluate whether the values of α_{MV} and α_{INV} differed between experimental conditions. Additionally, we used a bootstrapping technique[33] to place confidence limits on the fit values of these parameters. Details of these statistical procedures are described in the **Supplementary Note**.

Note: Supplementary information is available on the Nature Neuroscience website.

ACKNOWLEDGMENTS

The authors thank M. Kurgansky and L. Osborne for helpful comments on the manuscript and H. Gutierrez for technical assistance. This research was supported by a McKnight Scholar Award, the National Eye Institute (R01 EY15679-01A2), and the Howard Hughes Medical Institute Biomedical Research Support Program grant #5300246 to the UCSF School of Medicine. S.J.S. was supported by a National Science Foundation Fellowship.

COMPETING INTERESTS STATEMENT

The authors declare that they have no competing financial interests.

Received 5 January; accepted 25 February 2005
Published online at http://www.nature.com/natureneuroscience/

1. Welch, R.B., Widawski, M.H., Harrington, J. & Warren, D.H. Examination of the relationship between visual capture and prism adaptation. *Percept. Psychophys.* **25**, 126–132 (1979).
2. Ghahramani, Z. *Computation and Psychophysics of Sensorimotor Integration*. Thesis, Massachusetts Institute of Technology, (1995).
3. Jacobs, R.A. Optimal integration of texture and motion cues to depth. *Vision Res.* **39**, 3621–3629 (1999).
4. van Beers, R.J., Sittig, A.C. & van der Gon, J.J.D. Integration of proprioceptive and visual position-information: an experimentally supported model. *J. Neurophysiol.* **81**, 1355–1364 (1999).
5. Ernst, M.O. & Banks, M.S. Humans integrate visual and haptic information in a statistically optimal fashion. *Nature* **415**, 429–433 (2002).
6. Sober, S.J. & Sabes, P.N. Multisensory integration during motor planning. *J. Neurosci.* **23**, 6982–6992 (2003).
7. Soechting, J.F. & Flanders, M. Sensorimotor representations for pointing to targets in 3-dimensional space. *J. Neurophysiol.* **62**, 582–594 (1989).
8. McIntyre, J., Stratta, F., Droulez, J. & Lacquaniti, F. Analysis of pointing errors reveals properties of data representations and coordinate transformations within the central nervous system. *Neural Comput.* **12**, 2823–2855 (2000).
9. Flash, T. & Hogan, N. The coordination of arm movements: an experimentally confirmed mathematical model. *J. Neurosci.* **5**, 1688–1703 (1985).
10. Atkeson, C.G. & Hollerbach, J.M. Kinematic features of unrestrained vertical arm movements. *J. Neurosci.* **5**, 2318–2330 (1985).
11. Uno, Y., Kawato, M. & Suzuki, R. Formation and control of optimal trajectory in human multijoint arm movement: minimum torque-change model. *Biol. Cybern.* **61**, 89–101 (1989).
12. Gordon, J., Ghilardi, M.F., Cooper, S.E. & Ghez, C. Accuracy of planar reaching movements. 2. Systematic extent errors resulting from inertial anisotropy. *Exp. Brain Res.* **99**, 112–130 (1994).

13. Kalil, R.E. & Freedman, S.J. Intermanual transfer of compensation for displaced vision. *Percept. Mot. Skills* **22**, 123–126 (1966).
14. Wallace, B. & Redding, G.M. Additivity in prism adaptation as manifested in intermanual and interocular transfer. *Percept. Psychophys.* **25**, 133–136 (1979).
15. DiZio, P. & Lackner, J.R. Motor adaptation to Coriolis force perturbations of reaching movements: endpoint but not trajectory adaptation transfers to the nonexposed arm. *J. Neurophysiol.* **74**, 1787–1792 (1995).
16. Sainburg, R.L. & Wang, J. Interlimb transfer of visuomotor rotations: independence of direction and final position information. *Exp. Brain Res.* **145**, 437–447 (2002).
17. Taub, E. & Goldberg, L.A. Prism adaptation: control of intermanual transfer by distribution of practice. *Science* **180**, 755–757 (1973).
18. Cohen, M.M. Visual feedback, distribution of practice, and intermanual transfer of prism aftereffects. *Percept. Mot. Skills* **37**, 599–609 (1973).
19. Choe, C.S. & Welch, R.B. Variables affecting intermanual transfer and decay of prism adaptation. *J. Exp. Psychol.* **102**, 1076–1084 (1974).
20. Kitazawa, S., Kimura, T. & Uka, T. Prism adaptation of reaching movements: specificity for the velocity of reaching. *J. Neurosci.* **17**, 1481–1492 (1997).
21. Warren, D.H. & Schmitt, T.L. On plasticity of visual-proprioceptive bias effects. *J. Exp. Psychol. Hum. Percept. Perform.* **4**, 302–310 (1978).
22. Welch, R.B. & Warren, D.H. Immediate perceptual response to intersensory discrepancy. *Psychol. Bull.* **88**, 638–667 (1980).
23. Andersen, R.A., Snyder, L.H., Bradley, D.C. & Xing, J. Multimodal representation of space in the posterior parietal cortex and its use in planning movements. *Annu. Rev. Neurosci.* **20**, 303–330 (1997).
24. Wise, S.P., Boussaoud, D., Johnson, P.B. & Caminiti, R. Premotor and parietal cortex: corticocortical connectivity and combinatorial computations. *Annu. Rev. Neurosci.* **20**, 25–42 (1997).
25. Graziano, M.S.A. Where is my arm? The relative role of vision and proprioception in the neuronal representation of limb position. *Proc. Natl. Acad. Sci. USA* **96**, 10418–10421 (1999).
26. Graziano, M.S.A., Cooke, D.F. & Taylor, C.S.R. Coding the location of the arm by sight. *Science* **290**, 1782–1786 (2000).
27. Ghilardi, M.F., Gordon, J. & Ghez, C. Learning a visuomotor transformation in a local area of work space produces directional biases in other areas **73**, 2535–2539 (1995).
28. Rossetti, Y., Desmurget, M. & Prablanc, C. Vectorial coding of movement: vision, proprioception, or both? *J. Neurophysiol.* **74**, 457–463 (1995).
29. Goodbody, S.J. & Wolpert, D.M. The effect of visuomotor displacements on arm movement paths. *Exp. Brain Res.* **127**, 213–223 (1999).
30. Sainburg, R.L., Lateiner, J.E., Latash, M.L. & Bagesteiro, L.B. Effects of altering initial position on movement direction and extent. *J. Neurophysiol.* **89**, 401–415 (2003).
31. Jordan, M. Computational aspects of motor control and motor learning. in *Handbook of Perception and Action: Motor Skills* (eds. Heuer, H. & Keele, S.) (Academic, New York, 1996).
32. Good, P. *Permutation Tests. Springer Series in Statistics* 2nd edn. (Springer-Verlag, New York, 2000).
33. Efron, B. & Tibshirani, R.J. *An Introduction to the Bootstrap* (Chapman and Hall, Boca Raton, Florida, 1993).